

RECENT PROGRESS ON THE DIAMOND AMPLIFIED PHOTO-CATHODE EXPERIMENT*

Xiangyun Chang, I. Ben-Zvi, A. Burrill, J. Grimes, T. Rao, Z. Segalov, J. Smedley, BNL, Upton NY 11973, U.S.A.

Qiong Wu, Indiana University, Bloomington, IN 47405, U.S.A.

Abstract

We report recent progress on the Diamond Amplified Photo-cathode (DAP). The use of a pulsed electron gun provides detailed information about the DAP physics. The secondary electron gain has been measured under various electric fields. We have achieved gains of a few hundred in the transmission mode and observed evidence of emission of electrons from the surface. A model based on recombination of electrons and holes during generation well describes the field dependence of the gain. The emittance measurement system for the DAP has been designed, constructed and is ready for use. The capsule design of the DAP is also being studied in parallel.

INTRODUCTION

The DAP concept was first proposed a few years ago [1] and is under development now [2] [3]. The DAP has many advantages compared to the existing photo-cathodes. It requires 2 orders less laser power, has ultra high peak and average current capability, has ignorable contamination problem with the capsule design and is expected to have long lifetime.

The physical process of the DAP can be described by the following 5 steps: step 1: the primary electrons are generated by the conventional photo-cathode. These electrons are then accelerated to about 10keV energy by DC voltage to strike a diamond window with a thin metal coating on it. Step 2: the primary electrons penetrate the metal coating with some energy loss and generate a cascade of electron-hole pairs near the diamond surface. The number of pairs generated depends on the primary electron energy and is typically a few hundred. Step 3: the electron-hole pairs separates under the influence of the RF electric field (at the right phase) in the RF cavity accompanying with electron-hole recombination. Step 4: the secondary electrons drift through the diamond to the hydrogenated surface and the holes drift to the metal coating and recombine with replenishment electrons. Step 5: the secondary electrons are emitted from the Negative Electron Affinity (NEA) diamond hydrogenated surface and are accelerated by the RF field.

The following section identifies the issues related to each of the steps. The source of the primary electrons in Step 1 needs to be chosen and the capsule be designed carefully, taking into account the total current required by the device and vacuum level needed by the primary cathode.

Step 2 is straight forward and has no question.

In step 3 one needs to evaluate the electron transport properties carefully, taking into account all the scattering processes including the e-h recombination present in bulk diamond.

Step 4 requires high purity single crystal diamond or polycrystalline diamond with large grains to eliminate/reduce the trap centers in the bulk diamond. Synthetic diamonds meeting this criteria are now grown by the CVD technique and are readily available commercially.

In step 5, one needs to hydrogenate the sample to produce NEA surface. As the diamond surface has many surface states due to the lattice discontinuity, the secondary electrons may be trapped even on a well hydrogenated surface. We need to develop a way to reduce the trapping effect.

The emittance of the DAP in another important parameter for its applications. It is estimated that the thermal energy of the DAP electrons is about 0.4eV [4]. We've designed and constructed a system capable of measuring this small emittance [5].

EXPERIMENT RESULTS

Fig. 1 and fig. 2 are the schematic layout of the experimental arrangement for measuring the gain in the transmission mode and the emission mode respectively. In the transmission mode the diamond is metalized on both faces and after transmission through the diamond, the electrons are conducted away by the metal. In the emission mode, there is a gap between the diamond and the anode, and the electrons are emitted from the hydrogenated diamond surface in to the vacuum, to be transported to the anode.

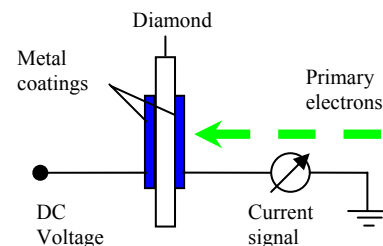


Figure 1: Electron transmission mode of the DAP.

The diamond samples are high purity single crystal diamonds with dimension of 4mm × 4mm × 0.3mm (Harris International detector grade diamonds).

For the transmission mode measurements, the sample is chemically etched first and then metalized on both sides with 15nm of Ti followed by 25nm of Pt.

*Work supported by the U.S. Department of Energy, and the Office of Naval Research.

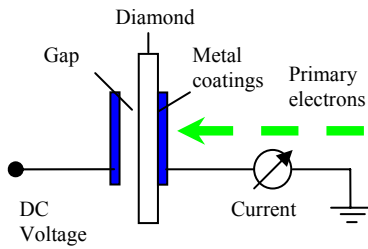


Figure 2: Electron emission mode of the DAP.

In the emission mode we coat one side of the diamond first with the same procedures above and then hydrogenate the other side.

The electron gain as a function of the electric field in the diamond for various primary electron energies is shown in fig. 3.

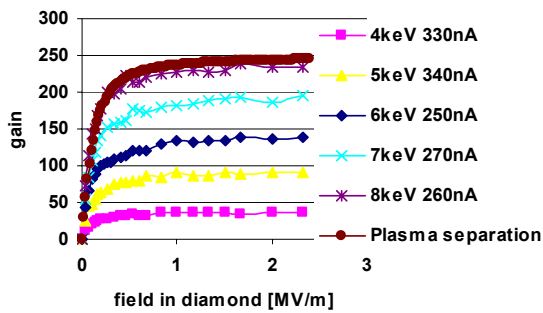


Figure 3: gain vs. electric field in diamond. The primary electron spot size is about 4mm².

The electron gain as a function of the electric field in the diamond for various primary electron energies is shown in fig. 3. The primary electron spot size is about 4mm²

Fig. 3 shows clear saturation behavior of the gain curve above 0.5MV/m field gradient for all primary electron energies. The maximum gain of each curve as a function of the primary electron energy is plotted in fig. 4. The trend line crosses at 3.3keV on x-axis indicating that the primary electron energy loss in the metal coating is about 3.3keV. The slope of the curve represents the energy loss in the diamond to generate one electron-hole pair and is found to be 20eV in this measurement. This number is slightly higher than what is reported before (~15eV). Probably this is due to the recombination effect during the charge separation.

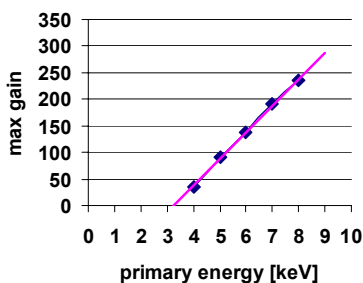


Figure 4: Maximum gain vs. primary electron energy.

The gain curve of the 8keV primary electron energy at 260nA was fitted with the charge separation model which is based on the following assumptions: the recombination rate is proportional to the product of the electron density and the hole density which are in turn proportional to the primary electron density. The electron and hole drift velocity v_d vs. electric field is expressed as [6]:

$$v_d = \frac{\mu_0 F}{[1 + (\mu_0 F / v_s)^\gamma]^{1/\gamma}}$$

where $\mu_0 = 2000 \text{ cm}^2 / \text{Vs}$ is the mobility at low field and is assumed to be the same for both electrons and holes. F is the electric field, $\mu_s = 1.1 \times 10^5 \text{ m/s}$ is the saturation drift velocity and $\gamma = 1$ is the fitting parameter.

The charge separation model describes very well the single primary electron case, which will apply to multiple primary electrons up to a very high number. This can be explained by the following simple estimation: due to the high mobility of the charge carriers and high saturation drift velocity, the time that each charge separation event can be as short as a few ps if the field is higher than 1 MV/m. The dimension of the secondary charge cloud is of the order of a few hundred nm, comparable to the primary electron stopping distance. Hence for all current densities $< 10 \text{ mA/mm}^2$, the secondary charge cloud from individual primary electrons do not overlap and the gain curve should be independent of the charge density and single primary electron model could describe the recombination process effectively. This limit is enough for most of the applications which require ultra high current density.

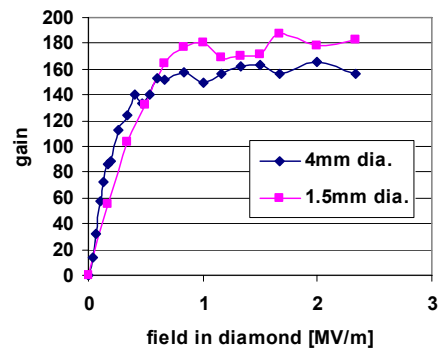


Figure 5: Gain vs. field curves with the same current but different spot sizes. Primary electron energy is 6keV and the current is 4.5µA.

Fig. 5 represents the gain vs. field curves with nearly one order of magnitude difference current densities. The gains at high field for the two cases are identical within the experiment error.

Fig. 6 shows the typical current signal we observed in the emission mode measurement. The primary electron pulse width is the same as the signal width. The 5µs plateau at the beginning of the pulse indicates that the trapping of the electrons near the hydrogenated surface are balanced by the emission of the electrons so that the electric field in diamond is constant. Later the trapping

dominates and the field in diamond decreases therefore the signal drops.

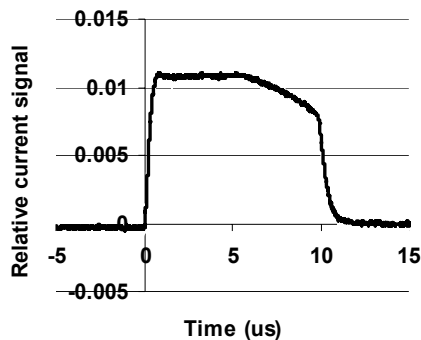


Figure 6: Current signal in the emission mode (4keV primary electron energy, 2.8MV/m field in diamond)

The strong trapping effect indicated by fig. 5 is possibly due to the small positive electron affinity of the hydrogenated surface because the lattice surface-normal orientation is $\langle 100 \rangle$ instead of $\langle 111 \rangle$. Another possible reason is that there are too many surface states on the hydrogenated surface.

Possible ways to overcome this trapping problem can be:

- Working at cryogenic temperature which can greatly reduce the probabilities of the electrons being trapped.
- Use $\langle 111 \rangle$ orientation single crystal diamond to have a real Negative Electron Affinity surface.
- Terminate the surface with alkali elements such as sodium or even potassium instead of the hydrogen.
- Gently treat the surface by the ion etching or laser ablation techniques.
- Use low energy laser to detrapp the trapped electrons.



Figure 7: Photograph of the new test chamber to measure the temperature dependence and emittance of DAP

Fig. 7 is the new test chamber that has been recently designed and constructed. This system is capable of measuring the sample at cryogenic temperature or high temperature. It is also designed to measure the DAP emittance.

CONCLUSIONS

Among the 5 stage sub-processes of the DAP operation described above, the first stage needs ultra high vacuum and can be solved by the capsule design. The second stage has no problem. The third stage has no problem for practical applications. The fourth stage needs single crystal pure diamond and probably with $\langle 111 \rangle$ lattice orientation. Only the fifth stage needs more investigations and we've proposed many possible solutions. This novel new type of photo-cathode is very promising.

REFERENCES

- [1] I. Ben-Zvi, X. Chang, P. D. Johnson, J. Kewisch, and T. Rao, "Secondary emission enhanced photoinjector", C-AD Accelerator Physics Report C-A/AP/149, Brookhaven National Lab, 2004.
- [2] X.Y. Chang, I. Ben-Zvi, A. Burrill, P.D.J. Johnson, J. Kewisch, T. Rao, Z. Segalov, Y. Zhao, "Study of Secondary Emission Enhanced Photoinjector", Proceedings PAC'05, Knoxville Tennessee, May 16-20 2005. p. 2711, <http://www.jacow.org>.
- [3] X.Y. Chang, I. Ben-Zvi, A. Burrill, S. Hulbert, P.D.J. Johnson, J. Kewisch, T. Rao, Z. Segalov, J. Smedley, Y. Zhao, "Measurement of the Secondary Emission Yield of a Thin Diamond Window in Transmission Mode", Proceedings PAC'05, Knoxville Tennessee, May 16-20 2005, p. 2251, <http://www.jacow.org>.
- [4] Xiangyun Chang, "Studies in Laser Photo-cathode RF Guns", Ph. D thesis, <http://www.bnl.gov/cad/ecooling/docs/PDF/Thesis/ThesisChang.pdf>
- [5] Q. Wu, I. Ben-Zvi, A. Burrill, X. Chang, D. Kayran, T. Rao, J. Smedley, "Thermal emittance measurement design for diamond secondary emission", Proceedings PAC'07, Albuquerque, New Mexico, June 25-29, 2007
- [6] Tomokatsu Watanabe, Tokuyuki Teraji, and Toshimichi Ito, "Monte Carlo simulations of electron transport properties of diamond in high electric fields using full band structure", Journal of Applied Physics, V. 95, number 9, p. 4886.